ON STRAIN-RATE SENSITIVITY AND SIZE EFFECT OF BRITTLE SOLIDS: TRANSITION FROM COOPERATIVE PHENOMENA TO MICROCRACK NUCLEATION

Sreten Mastilovic

Union - Nikola Tesla University, Faculty of Construction Management, Cara Dusana 62-64, 11000 Belgrade, Serbia

E-mail: smastilovic@fgm.edu.rs

Abstract

An idealized brittle microscale system is subjected to dynamic uniaxial tension in the medium-to-high strain rate range ($\dot{\varepsilon} \in [100\, s^{-1}, 1\times 10^{7}\, s^{-1}]$) to investigate its mechanical response under constrained spatial and temporal scales. The setup of dynamic simulations is designed to ensure practically identical in-plane stress conditions on a system of continuum particles forming a two-dimensional, geometrically and structurally disordered, lattice. The rate sensitivity of size effects is observed as well as the ordering effect of kinetic energy. A simple phenomenological expression is developed to account for the tensile strength sensitivity of the small-sized brittle systems to the strain-rate and extrinsic size effects, which may serve as a guideline for formulation of constitutive relations in the MEMS design. The representative sample is defined as a square lattice size for which the tensile strength becomes rate-insensitive and an expression is proposed to model its evolution between two asymptotes corresponding to the limiting loading rates. The dynamics of damage accumulation is analyzed as a function of sample size and loading rate.

Keywords: lattice models, brittle solids, disordered system, representative volume element, size effect, strain-rate effect, scaling exponents.

1. INTRODUCTION

The continuing demand of modern technologies for miniaturization of structural elements drives a need for understanding the complexities and specificities of materials dynamic response at small length scales. A surge of research activity in the past decade related to study of inelastic behavior of the confined dimensions has been initiated by Uchic and coworkers [26] who reported strong size effects on the compressive yield strength of micrometer sized single crystals for three different Ni-based materials. The cylindrical specimen (called micropillars) have been manufactured by focused ion beam (FIB) machining and then compressed by using a conventional nanoindentation device outfitted with a flat-tip indenter. Greer and Nix [27] extended this methodology into the nanoscale regime where single crystalline Au nanopillars achieved strength that was significant fraction of theoretical strength. Several research groups applied the same testing methodology to investigate

the size effect on compressive strength of ductile, predominantly face-centered cubic, materials [e.g., 28-30]. More recently, this ingenious experimental technique has been adapted to the uniaxial tensile experiments (essentially by introduction of nanointender grips) [e.g., 31-33] inherently more difficult to perform. Various aspects of plasticity in confined dimensions have been investigated both analytically and computationally [e.g., 36-39] (and references therein). The comprehensive reviews of the testing performed by this elegant methodology and the corresponding intensive research efforts were presented annually in the last few years [33-36]. Since the finite element method is still the workhorse of the structural and failure analysis, these fascinating developments concerning the material response at small spatial and temporal scales (for the latter consult, for example, Bourne [52]) highlight the issue of representative volume element (RVE).

The concept of RVE is an essential building block of micromechanics and its definition is "perhaps one of the most vital decisions that the analyst makes" [13]. Introduced by Hill [50] to express systematically and rigorously the relation of material's microstructure and its macroscopic response, it represents a volume of heterogeneous material statistically representative of certain local continuum property at the corresponding material point (for detailed discussion and list of references see, for example, [8] or [13]). A systematic definition of the RVE with respect to the considered property is a problem-specific task since only the relative dimensions with respect to the "underlying essential microconstituents" [13] are of concern. In the lattice models the size of RVE is defined by the correlation length yielded by the analysis of consecutively breaking links in the course of damage evolution [25]. Krajcinovic and Rinaldi [5] defined it as "the smallest specimen volume, of disordered matter, that is statistically homogeneous", that is, translationally invariant. For the purpose of the present investigation, the size of RVE with respect to the uniaxial tensile strength is tentatively identified with the sample size corresponding to the rate-insensitive tensile strength for the given level of microstructural disorder.[1] This approach offers insight in appropriateness of the use of various maximum normal stress theories in the finite element analysis (FEA).

The continuum models of inelastic material behavior are still largely of phenomenological type. This is especially apparent in the case of the continuum damage models and high-

[1] The breakdown thresholds are—unlike the transport properties—commonly considered to be extrinsic to brittle materials "since they as a rule depend on the specimen volume" [8]. Nonetheless, the present approach is inspired by an observation of certain regularity of the lattice strength behavior (most notably, the sample-size thresholds of rate-insensitive strength) and a number of theories of the size dependence of the nominal strength starting from the Griffith's classical work in 1920's; a comprehensive summary is presented, for example, by van Vliet [41]. The historical survey of the high strain rate techniques in general, and the recommendations regarding the choice of mechanically representative specimen size in particular, are available in [51] and references cited therein. The specimen representativeness is at the core of problem of transferability of results from specimen to, for example, the rock massif or concrete structure. The term "extrinsic size effect" [36] was introduced to account for the "smaller is stronger" (sample-size related) phenomenon ubiquitously observed in metallic structures on the micron and submicron scales; the "intrinsic size effect" is related to the materials' microstructure.

deformation-rate models. These models are based on the principles of determinism and local action, material objectivity and invariance [8], have to satisfy the conservation laws and the second law of thermodynamics, and include constitutive relations. Models traditionally used in commercial FEA codes are, more often than not, based on class of empirical constitutive laws of the following form:

$$\bar{\sigma} = f(\bar{\varepsilon})g(\dot{\bar{\varepsilon}})h(T) \tag{1}$$

where bar above symbols denotes the volume averages over RVE. The classical homogenization techniques are not designed to account for size effects on the effective mechanical response of heterogeneous material [13,24]. Nonetheless, although the limits of the traditional damage mechanics models are discussed at length in literature (e.g., [5,8]), the higher-gradient theories offer interpretation of the corresponding homogenized models in terms of the underlying discrete models (e.g. [21]) and insights into their mechanical properties.

2 SIMULATION MODEL

The present computational method is an offspring of a particle modeling (an engineering offshoot of molecular dynamics [20]) and spring-network models of the central-force type. Thus, it is a simple two-dimensional network of springs with frictionless hinges at the nodal points (continuum particles), designed with a specific aim to facilitate an objective comparison of some underlying aspects of dynamic response of the low-fracture energy systems [10,11,20]. The microscale sample is comprised of an idealized brittle material approximated by a disordered two-dimensional structure: a Delaunay simplicial graph dual to an irregular honeycomb system of Voronoi polyhedra representing, for example, grains of a ceramic material. In general, the identification of the microconstituent that dominates the macroresponse (the intrinsic size effect) depends on the particular problem and particular objective [13,19]. In the present framework:

i. grain boundaries ("the most common examples of weak interfaces in brittle materials" [53]) are considered to provide the direct, first-order effects on the overall dynamic response (entirely grain-boundary mediated);
ii. the average grain diameter is the texture parameter that defines the model resolution length, l_c, while the grain size and grain boundary stiffness distributions define the intrinsic size effect;
iii. other microheterogeneities and defects (resulting in the local stress and strain fluctuations) on a smaller scale ($\xi < l_c$) are accounted for by stiffness and strength distributions [8]; and

iv. thermal vibration effects, other than the mechanical vibrations of the system of coupled oscillators itself, are not taken into account for the sake of model simplicity.

Within this model framework, the microstructural texture is represented by a network of grain boundaries while the cracking is necessarily intergranular. The size of grains and strength of grain boundaries in a polycrystalline ceramics are distinctively stochastic parameters. This inherent aleatory variability is further enhanced by the nucleation-dominated damage evolution governed by the local fluctuations of stress and quenched energy barriers [10].

The continuum particles located in lattice nodes interact with their nearest neighbors through the nonlinear central-force links (stemming from the Hook potential in tension and the Born-Meyer potential in compression). The coordination number z (defined as the number of nearest neighbors of a bulk particle) and initial link length λ_0 define the randomness of the lattice morphology. The lattice is geometrically and structurally disordered since the equilibrium distances between particles (in the pristine configuration) and their mutual link stiffness are sampled independently from the normal and uniform distributions, respectively, within the ranges $\alpha\,\overline{\lambda} \le \lambda_0 \le (2-\alpha_l)\,\overline{\lambda}$ and $\beta\,\overline{k} \le k \le (2-\beta_l)\,\overline{k}$. The geometrical-order and structural-order parameters $(0 \le \alpha_l \le 1)$ and $(0 \le \beta_l \le 1)$ respectively define the bandwidth of the geometrical disorder and stiffness distribution [10,20]. The link-rupture criterion is defined in terms of the critical link elongation $\varepsilon_{cr} = const.$ such that the link between particles i and k ruptures when its elongation reaches the critical value $\Delta\lambda_{ik} = \varepsilon_{cr}\,\lambda_{0ik.}$

The model thus described recognizes, in general, two different types of inter-particular links: chemical and mechanical. Chemical links are limited to the nearest neighbors while the number of particles interacting by mechanical contact is unlimited. Although this model feature is crucial for some deformation histories (e.g., the flow of comminuted phase in the course of the cylindrical cavity expanding in brittle material [20]) it is not that important in the present simulation.

The unnotched tensile specimen represents a polycrystalline micropillar of square shape (aspect ratio $L/D = 1$) with side length D.[2] The problems of the uniform load distribution and the loading at high rates are solved by imposing a computational artifice: an instantaneous initial velocity field to the lattice in the loading direction, $\dot{x}_1(t=0) = \dot{\varepsilon}_1\,x_1$, and perpendicular to it, $\dot{x}_2(t=0) = -\upsilon_0^{(\varepsilon)}\,\dot{\varepsilon}_1\,x_2$, defined in the terms of the prescribed strain rate, $\dot{\varepsilon}_1 = \dot{L}/L$ and the apparent plane-strain Poisson's ratio of the pristine material, $\upsilon_0^{(\varepsilon)}$ [18]. Subsequently, at $t > 0$, only

[2] The effect of aspect ratio on the compressive uniaxial test is well understood and amply documented in literature (e.g., [30]). The recent experiments [31] reveal also significant difference in size effect in *tension* depending on the sample aspect ratio: both the size effect and hardening were, due to constrained glide and corresponding dislocation pile-ups, much more pronounced for the samples with L/D=1 compared to those with high aspect ratio.

velocity of the particles located at the longitudinal boundaries ($x_1 = \pm L/2$) is controlled, $\dot{x}_1 = \pm \dot{\varepsilon}_1 \, L/2$; motion of all other particles is governed by Newton's equation of motion, discretized in time and integrated using one of many finite-difference algorithms to obtain the particle trajectories. The far-reaching effects of this loading procedure are described in [10].

The parameters recorded through the entire process are: the position and velocity of each particle, number of ruptured links, and force in each link. Calculation of the kinetic and damage parameters, knowing the position and velocity of each particle and inter-particular link statistics, is straightforward. For example, the damage energy is calculated as $E_D = \sum k \, \varepsilon_{cr}^2 \, \lambda_0^2 \, /2$, where summation is performed over all broken links (indices are omitted for brevity). The statistical mechanics expressions for the components of the stress tensor are adopted from the molecular dynamics ([10], [20]):

$$\sigma_{\alpha\beta} = \frac{1}{2LD} \sum_{\substack{i,\,k \\ i \neq k}} \frac{d\varphi(\lambda_{ik})}{d\,\lambda_{ik}} \frac{(\lambda_{ik})_\alpha \, (\lambda_{ik})_\beta}{|\lambda_{ik}|} \tag{2}$$

where $(\lambda_{ik})_\alpha$ is the α-component of the vector $\vec{\lambda}_{ik} = \vec{r}_i - \vec{r}_k$, $\vec{r}_i$ the position vector defining the location of i-th particle, $\varphi(\lambda_{ik})$ the pair potential, and LD the sample "volume"; the alphabetic indices refer to particular lattice particles, while the Greek letter subscripts are reserved for tensor components.

The tensile test simulations are performed at seven different strain rates: 100 s^{-1}, 1×10^3 s^{-1}, 1×10^4 s^{-1}, 1×10^5 s^{-1}, 3×10^5 s^{-1}, 1×10^6 s^{-1}, 1×10^7 s^{-1}. For the reason of computational economy, only a single realization is performed for eight lattice sizes (see Fig. 6) distributed over the wide range $D/l_c \in [9, 765]$, fulfilling, therefore, the requirement that "the RVE must be several orders of magnitude larger than the size of its microconstituents" [13]. Additionally, in order to evaluate the size-effect on the strength data scatter, ten repeated realizations are performed for selected lattice sizes (see Table 1 for specifics) by using different statistical realizations of the geometrical and structural disorder for the same $(\dot{\varepsilon}, D)$ pair.

The procedures for constructing a mechanically equivalent lattice capable of matching the physical properties of polycrystalline ceramics are developed by Rinaldi et al. [16]. Nonetheless, since the quantitative estimate of the material's mechanical response is beyond the objective of the present study, no attempt is made to calibrate the major statistics of the given microstructure. The geometric and structural lattice parameters are: the coordination number $z = 6$, the average equilibrium distance between particle sites $\overline{\lambda} = 1$, the average link stiffness $\overline{k} = 8E_0/5\sqrt{3}$ (where

E_0 is the modulus of elasticity of pristine material), the geometrical-order parameter $\alpha_l = 1/5$, the structural-order parameter $\beta_l = 2/3$, and the rupture strain of the links $\varepsilon_{cr} = 0.35\%$ (applied everywhere except within an elastic frame of thickness $2\,l_c$ introduced to reduce data scatter that might be caused by edge effects in the highly brittle system). The discussion of reduced units is available in [10] or [20]. These reduced units are scaled herein to correspond to alumina (Al_2O_3) with the average grain diameter $l_c = 10$ μm and velocity of elastic longitudinal wave propagation $C_L \approx 10$ km/s. It should be emphasized that this is done for scaling purposes only – the lattice itself is not aimed at capturing of the behavior specificities of any real brittle material.

Although the selected lattice modeling approach was validated in the past on a series of benchmark problems (e.g., [20]), the inherent shortcomings of material representation by the triangular central-force lattices, discussed in detail in the past (e.g. [9,19,40]), should be noticed. Nonetheless, we believe that these important issues (e.g., the fixed Poisson's ratio, relatively high anisotropy, artificial macrocrack bridges) have only second-order effects on rather qualitative results of the present study, bearing in mind motivation of the work and the specific numerical simulation setup. It is well known that the lattice models of this type are best suited when applied to systems of the similar topology. The present basic lattice model is admittedly crude and not as adequate for the polycrystalline ceramics as for, say, a cellulose fiber network [47] or two-phase particulate composites [19]; but, nonetheless, its application does not represent mere discretization of continuum but rather reflects the discrete and disordered nature of the materials whose failure is governed by a web of weak interfaces. The bond-bending model (e.g., [9,47]) would be a better suited for the study of fracture propagation but at the cost of considerably more computation time. As Jagota and Bennison [40] concludes regarding the deficiencies of central-force model: "This may not be an issue when dealing with the large disorder and when the goal is to study universal scaling relationships…" In is also important to emphasize that the results presented herein refer to the stress-peak parameters and, therefore, are not affected by a complex phenomena in the softening regime, which are clearly more demanding from the modeling standpoint.

A comprehensive review of lattice models in micromechanics is presented by Ostoja-Starzewski [47]. Finally, the recent advances in using discrete element models to simulate the dynamic loading of concrete ([44,46] and references therein) should not be overlooked in the present context.

3. RESULTS AND DISCUSSION

The stress peak neighborhood and the softening regime are aspects of the brittle response that deserve a careful scrutiny. The state of damage at that critical point (stress peak), marking the onset

of homogeneous-heterogeneous transition [15], and various aspects of post-critical behavior depend on the loading rate but also on the intrinsic and extrinsic size effects. The lattice damage patterns (illustrated in Fig. 5 as typical examples for the three loading rate regions) and stochastic effects of microstructural disorder on damage growth are discussed in [10,11,23]. Most notably, these simulation results suggest that with the strain rate decrease from the extremely high ($\log \dot{\varepsilon} \geq 6$) to the high ($4 < \log \dot{\varepsilon} < 6$), the size of a typical flaw (l_f)—emerging in the softening regime—changes gradually from minuscule clusters comprised of a couple of broken links ($l_f \approx 1 \div 5\ l_c$) to the large complex microcrack clouds whose characteristic linear length exceeds dozens of intrinsic microstructural lengths. The reduction of the loading power continuously coarsens the web of microcrack clouds in terms of both the typical cluster size (l_f) and their mutual distance (Fig. 5; e.g. [23] for more details). This trend reflects transition of the dominant damage evolution mechanism from the microcrack nucleation (at the extremely high strain rates) to the cooperative phenomena among microcrack clusters (at the high strain rates). The following inequalities

$$l_c \leq l_f << L_{rve} < D, \qquad \forall\ \dot{\varepsilon}[s^{-1}] \ni \log \dot{\varepsilon} \geq 6 \tag{3a}$$

$$l_c < l_f < L_{rve} \leq D, \qquad \forall\ \dot{\varepsilon}[s^{-1}] \ni 4 < \log \dot{\varepsilon} < 6 \tag{3b}$$

between the characteristic lengths during that strain-rate reduction, are suggested by the simulation results, and since the area (volume) of the damaged brittle material exhibits invariance with respect to the translation it is considered statistically homogeneous.[3]

Finally, in the limit case of the quasi-static tensile loading (which is outside of the present work scope), a material microstructure, containing many randomly distributed microcracks, is initially statistically homogeneous (hardening region), but becomes heterogeneous (softening region) due to localization of microcracks and their clustering into a dominant macrocrack of length commensurate with the sample size [42]. The failure threshold is reached when the macrocrack length reaches the correlation length equal to the sample size ($l_f \approx D$) [5,15,20]. The brittle response is such that the expectation of a continuous random variable depends strongly on the position within the sample, rendering the mean field models unsuitable. The translational invariance disappears, the damaged material ceases to be statistically homogeneous, and the RVE with respect to the tensile strength does not exist.

[3] Translational invariance implies that the macro-parameters depend only on the density of micro-elements but not on their positions within the sample [5].

3.1. Strain rate effects on sample size strength dependence

It is well known that the ultimate tensile strength of brittle materials is a rate-dependent stochastic property [11], which, as a rule, exhibits a dramatic extrinsic size effect. The usual trend, common for all spatial scales from macroscopic to microscopic, is that with the sample size increase, the stress peak decreases and gradually approaches the asymptotic value corresponding to the size-independent strength (e.g., [1-3], [41]). This ubiquitously observed behavior is in the case of low-fracture-energy materials often interpreted according to the Weibull statistics[4] and the probability of finding the "weakest link" within the sample. The experimental results of uniaxial compression of micro- and nanopillars indicate that their yield strength depends on pillar diameter in a power-law fashion, $\sigma_m \propto D^{-\zeta}$, with $0.5 \le \zeta \le 1$ [22]. More recent tensile experiments [31-33] unambiguously demonstrate a nearly identical extrinsic size effect in metallic small-scale structures.

The preceding studies by the same simulation method [10, 11, 23] offer an argument that the attainment of nearly theoretical strength (after practically elastic loading up to catastrophic failure) and the disappearance of both intrinsic and extrinsic size effects at the extremely high loading rates are attributable to the strain rate driven stochastic-to-deterministic transition of brittle response. Within the framework of the present computational model, this transition is evident in the reductions of: (i) the strength dispersion [10,11], (ii) the damage energy rate scatter in the softening phase [23], and (iii) stochasticity of the damage evolution patterns [23]; which are all attributed to the diminishing role of microstructural disorder in the brittle response.

The strain-rate sensitivity of small scale metallic systems is emerging recently [22] with observation that at the relatively low strain rates (less that 0.1 s^{-1}) strength size dependence deviates from the ubiquitously observed power law. Importantly, this crossover to the size-independent strength [28,30], markedly below the theoretical strength, takes place at very small pillar diameters (e.g., < 150 nm for the Cu monocrystalline nanopillars) and depends on the amount of dislocation sources in the ductile sample.

The ubiquitous size effects are observed in the present simulations as well. Additionally, the simulation results presented in Fig. 1 indicate the strain rate effects on the strength increase compared with the strength of unbounded brittle medium (i.e., the size-independent bulk strength).

The least-squares fit of the simulation results obtained for low-fracture-energy systems suggests

$$\sigma_m = \sigma_{m\Lambda} + \left(\sigma_m^{th} - \sigma_{m\Lambda}\right)\left\{1 - \exp\left[-\left(\frac{\log\dot{\varepsilon} - A}{B}\right)^C\right]\right\}, \qquad \log\dot{\varepsilon} \ge A \tag{4a}$$

[4] The non-applicability of the Weibull statistics to the sub-micrometer scale is emphasized in [36].

$$\sigma_{m\Lambda} = \sigma_{m0}\left(1 + S\,D^{-\varsigma}\right) \tag{4b}$$

where the lower asymptote σ_{m0} is the bulk quasi-static strength ($\log D \to \infty$ and $\log \dot{\varepsilon} \to A$); σ_m^{th} is the "theoretical strength"—the upper limit of the tensile strength—independent of the inherent and induced flaw structure and the size of the brittle system ([10,11]); the quasi-static threshold, A, and the parameter B, define of the onset of the rate-driven strength increase (from σ_{m0} to σ_m^{th}) whose gradient is defined by the model parameter C [11].

The functional dependence (4a) was inspired by the translated Weibull cumulative distribution function:

$$F(x) = 1 - \exp\left[-\left(\frac{x-\gamma}{\eta}\right)^{\beta}\right], \qquad x \geq \gamma \tag{5}$$

where γ, η, and β are the location, scale, and shape parameters, respectively, such that ($-\infty < \gamma < \infty$), $\eta > 0$, and $\beta > 0$ [48].

The Weibull distribution is widely applied to many random phenomena due to its extreme value behavior. The appropriate selection of distribution parameters allows close approximation of many observational phenomena. Notably, it has been recently used by Rinaldi [38] to develop first-order theory of the sample-size effect on the yield strength of nanoscale pillars. The median, one of commonly used statistics of central tendency of the data sample, in the case of the translated (3-point) Weibull distribution has the form:

$$M(X) = \gamma + \eta\,(\ln 2)^{1/\beta} \tag{6}$$

Consequently, it is obvious based on Eq. (4a) that for a fixed sample size ($D = Const.$) the "crossover" strain rate $\dot{\varepsilon}_{\times}$ corresponding to $\sigma_m = (\sigma_m^{th} + \sigma_{m\Lambda})/2$ [23] is by definition the median (6) (by analogy with the Weibull cumulative distribution function (5)), which offers the following relationship between the model parameters

$$B = \left(\log \dot{\varepsilon}_{\times} - A\right)(\ln 2)^{-1/C} \tag{7}$$

The tensile strength expression, Eq. (4), is an upgrade (of the previously developed strain rate model [11, 23]) of practical consequence in a sense that it may serve as a template to formulate constitutive relations for the MEMS design of brittle confined structures. The connection to the

Weibull distribution, Eqs. (5-7), is a novel, not fully explored, element, reconciling the strain rate effects to the traditionally accepted framework of the strength of materials.

Fig. 2 illustrates the effects of strain rate and sample size on the tensile strength of the quasi-brittle solids. The following limit cases should be observed for the unbounded medium

$$\lim_{\dot{\varepsilon}\to\infty}\left(\sigma_m\right)=\sigma_m^{th} \tag{8a}$$

$$\lim_{\dot{\varepsilon}\to 0}\left(\sigma_m\right)=\sigma_{m0} \tag{8b}$$

(Naturally, the strain rate has its finite upper bound determined by the Debye's atomic vibration period [14]; the lower bound, corresponding to the quasistatic loading, is in terms of Eq. (4a) formally identified with the location parameter A.) The advantage of Eq. (4a) over the empirical expression, $\sigma_m=\sigma_{m0}\,\dot{\varepsilon}^{m}$, typically used for data fitting of empirical constitutive laws of the form (1), is that it captures not only ubiquitous strength raise (e.g., a comprehensive compilation of concrete data [45]) but also the high-strain-rate plateau (σ_m^{th}) suggested by the shock experiments (for discussion, see [20] and references therein).

The studies of the joint effects of size and strain rate on steel properties by Morquio and Riera [43] established an existence of "a statistically significant interaction between size and strain rate that is particularly relevant in the tensile strength" and resulted in a new predictive expression, which fits the data rather well. Although the scope of the present study is limited to the highly brittle materials, the simulation results presented in Fig. 1 also suggest that the sample size driven strength evolution is strongly strain-rate dependent. From the standpoint of Eq. (4b), it may be tempting to assume the rate dependence of the scaling exponent: $\varsigma=\hat{\varsigma}\left(\dot{\varepsilon}\right)$ such that $\lim_{\dot{\varepsilon}\to\infty}\left(\varsigma\right)=0$. Nonetheless, the fitting of our simulation data with such strain-rate dependence proved somewhat strenuous undertaking, which agrees with suggestion by Jennings et al. [22] that the power-law slope of Cu nanopillars is not significantly affected by strain rate in the sub-micron regime. An obvious alternative was to assume strain-rate dependence of the multiplier S, which proved rather easy to fit. With exception of the obvious limit

$$\lim_{\dot{\varepsilon}\to\infty}\left(S\right)=0 \tag{9}$$

it seems of dubious utility to attempt to speculate on the functional form $S=\hat{S}\left(\dot{\varepsilon}\right)$. Nonetheless, it should be noted, based on the simulation results analysis, that the functional dependence is highly non-uniformly distributed over the strain-rate range, and seems to imply an abrupt change in the

transitional region (corresponding to the strength surge depicted in Fig. 2) - resembling qualitatively the strain-rate dependence of the representative sample size illustrated by Fig. 5. That evolution is characterized by a relatively weak rate dependence corresponding to very high and very low strain rates with the rapid decline in the transitory region towards the lower asymptote defined by Eq. (9).

It is also noteworthy that, contrary to the trend observed in single-crystalline Cu nanopillars [22], the strain-rate driven increase of tensile strength for brittle microsystem reduces with sample size reduction (Fig. 3). It cannot be overemphasized that Fig. 3 illustrates results of one single realization of microstructural statistics per $(D, \dot{\varepsilon})$ pair. It is, consequently, subject to inherent stochasticity not only in the case of smaller sample size (as illustrated in Fig. 4) but also due to the variability of response of disordered brittle media to low-strain-rate loading [23]. With reference to Fig. 4., the considerable strength-scatter decrease with increasing sample size is reminiscent of the strength-scatter decrease of Mo-alloy monocrystalline micropillars due to the increase of pre-strain and pillar size (concocting jointly increase of the amount of dislocation sources) that suggests "a transition from discrete to collective dislocation behavior" [28]. Naturally, the typical deformation mechanisms that dominate phenomenological behavior of ductile and brittle materials are substantially different (with widely different representative temporal and spatial scales of observation [52]) but the underlying nature of their appearance/behavior (such as discrete vs. collective) yields similar, if not universal, trends. Ubiquity of the observation that collective behavior promotes determinism renders it almost obvious.

Fig. 3 also demonstrates that with the sample-size increase, brittle response becomes insensitive to extrinsic size effect and, therefore, representative of the bulk behavior with respect to the tensile strength. The reduction of strain-rate sensitivity of tensile strength (m exponent in Fig. 3) with sample size reduction can be attributed to the spatial confinement, which is, under the framework of the present model, responsible for the strength surge in the transitory region in our opinion.

3.2. Sample size and strength data scatter

The brittle failure is a complex process influenced substantially by stochastic and random factors, and material disorder. As previously mentioned, the failure nucleation in, and the strength of, low-fracture-energy systems is driven by weak link considerations and the strength is therefore, to a various degree, an outcome of the Weibull process [4]. This extreme behavior implies that the strength is an extrinsic property [4]. In the case of a very small sample or a very low loading rate or both, the *highly* brittle system is prone to catastrophic ("avalanche") failure without substantial "quantized" propagation of damage [17] in the hardening regime. The damage tolerance is very

limited and the damage power in the softening (post-critical) regime is extremely high [23]. Behavior of such small-size system is sensitive to the weakest link principle, prone to "avalanche" failures [5,15], and its time-to-failure (although generally an outcome of a complex process of formation and evolution of dissipative structures [49]) may be affected by the lifetime of the weakest link to various extents depending on the details of "problem statement" [4]. Notably, the weakest links may rupture in an early stage of hardening regime with no noticeable consequence for even global lattice response, not to mention stability; but in the case of large local fluctuations of microstrain and microstrength fields, a rupture of one "favorable" link may serve as a nucleus for the rapid critical-cluster formation (and propagation and global failure). (Note the difference from the limit case of the perfectly brittle system governed strictly by the weakest link principle, where the lifetime of the system coincides with the lifetime of weakest link, thus, the first order statistic *determines completely* the life of the system [17,19,48].) Since the probability of finding a *weaker* link (or more "favorable" link–in the rupture sense discussed above) scales, for the given statistics, with the sample size, it is to be expected that the stochasticity of brittle response increases with the sample-size reduction. A large sample advances reduction of response scatter. This trend is illustrated by Fig. 4 and in Table 1, which present the basic statistics for $\dot{\varepsilon} = 1 \times 10^4\ s^{-1}$ simulations. The same qualitative trend is observed in the experimental data on steel type ASTM A36/96 obtained by Morquio and Riera [43]. The observed tendency of "vanishing" σ_m standard deviation with the sample-size increase implies the diminishing stochasticity (and, thus, the increased determinism) of the brittle response.

Table 1. *Basic data statistics of the size effect on the normalized strength increase (i.e., with respect to the bulk value) for $\dot{\varepsilon} = 1 \times 10^4\ s^{-1}$. D/l_c is non-dimensional size of the square sample defined as the ratio of the lattice length and the model resolution length identified with the average link length ($l_c = \overline{\lambda}$).*

	D/l_c [-]	9	23	51	93	765
$\overline{\sigma}_m$	MEAN	1.41	1.18	1.10	1.05	1.001
	STANDARD DEVIATION	0.18	.096	0.046	0.031	.0098

3.3. The strain rate dependence of the representative sample size

Fig. 1 illustrates that the stress peak size-dependence is qualitatively similar for all strain rates. The lattice size at which the stress-peak value becomes size independent is defined herein as the

representative sample and identified tentatively with the RVE with respect to the tensile strength (the shaded area in Fig. 1 corresponds to 2% deviance from the horizontal asymptote).

It is obvious from Fig. 1 that the gradient of the strength increase, and, consequently, the representative sample size, depend significantly on the strain rate. If the representative sample size corresponding to quasi-static loading is designated as L_r^0, its strain rate-driven evolution could be represented qualitatively by the function:

$$L_r = L_r^\infty + \left(L_r^0 - L_r^\infty\right)\exp\left\{-\left[\frac{\log\left(\dot{\varepsilon}\right) - P}{R}\right]^Q\right\} \tag{10}$$

where P, R, and Q are fitting parameters. The lower representative sample asymptote ($L_r^\infty << L_r^0$), corresponding to the ordered homogeneous mesoscale damage patterns [10] at the theoretically maximum strain rate [14], depends on the resolution length of the model l_c (i.e., it is individual for each microstructure). Physically, it appears reasonable to suppose that for the high-quality ceramics, such as titanium diboride or titanium carbide, L_r^∞ may be on submicrometer scale.

The typical damage patterns (depicted in Fig. 5 in association with the medium, transitory and extreme loading-rate ranges) provide a graphical interpretation of the representative sample size rapid decline described by Eq. (10), which appears inherently related to the necessity of changing observation scale to meet the translational invariance requirement (e.g., the stress-peak patters in [23]). Since the present spring lattice model cannot capture many significant physicochemical changes in material associated with high strain rates (e.g., [12]), these damage patterns are, necessarily, purely mechanical manifestations of the rate change reflected by the number and dynamic arrangements of broken bonds in a system of coupled oscillators under a specific loading setup. Nonetheless, the phenomenological expression (10) may prove to be of practical importance in the computational engineering since, for example, it may guide the experimental data fitting or extrapolation.

3.4. Effects of sample size and strain rate on damage evolution

The damage accumulation in brittle systems is especially important because the critical amount of damage necessary to cause failure can be not only limited but also difficult to detect. The number of broken bonds is the indicator of total microcrack density that, in the case of isotropic damage distribution, is sufficient for definition of the proper damage parameter (e.g., [8]). According to Hansen et al. [6], in the case the quasi-static loading of triangular spring networks, the number of broken bonds corresponding to the apex of the stress-strain curve (n_m) scales with lattice size with the scaling exponent 1.75; these authors obtained the same scaling exponent using the lattices of

square-arranged beams [7]. Delaplace et al. [25] reported a similar scaling exponent for the fuse lattices with square-arranged links. A list of the fractal dimensions of fracture surfaces in different phases of crack growth was compiled and discussed by Mishnaevsky Jr. [49].

In the present case

$$n_m \propto D^{\delta} \quad \forall\, \dot{\varepsilon} \tag{11}$$

but it appears, based on Fig. 6, that a continuous spectrum of rate-dependent scaling exponents is necessary for the complete description of the two-dimensional system

$$1 \le \delta = \hat{\delta}\left(\dot{\varepsilon}\right) \le 2 \tag{12}$$

Although the theoretical justification for the power-law behavior (11) is not fully available, it can be observed that the stress-peak damage (at time-to-failure $t \equiv t_m \propto \left(\varepsilon_{cr}\ \dot{\varepsilon}\right)^{-1}$, [23]) in the dynamically loaded disordered brittle lattice—described apparently by the continuous spectrum of scaling exponents—reflects its predominant distribution arrangement as illustrated by the damage patterns in Fig. 5. In fact, at smaller strain rates, as the failure pattern tends to a localized nearly-straight fracture, the exponent approaches the lower bound ($\delta = 1$), whereas it increases progressively towards the upper bound ($\delta = 2$) as damage becomes a more uniform process of microcrack nucleation extending over the entire lattice area for high strain rates. The scaling exponent crossover from the lower to the upper horizontal asymptote takes place primarily in the transitory region as indicated by slopes in Fig. 6. Thus, the upper bound ($\delta = 2$), corresponding to the extremely high strain rates, may be interpreted as a fat fractal typically describing damage accumulation driven by the random nucleation of microcracks. As argued by Rinaldi et al. [12]: "a fractal exponent close to one makes intuitive sense for the invariant set driving the *propagation*,[5] as much as a fat fractal suits the phenomenology of the *nucleation*".

4. CONCLUSIONS

Although the plasticity in small-sized crystalline metallic materials is extensively tested in the last few years, the similar experimental data is apparently not available yet for the brittle materials such as ceramics. The uniaxial tension simulations employed herein provide insight into effects of high strain rates and small dimensions on the mechanical behavior of an idealized low-fracture-energy microsystem under a specific loading setup. From the standpoint of the weakest link principle, existence of the representative sample (characterized by the size-insensitive strength), for the given

[5] Also, refer to [49] for more details on this class of fractal dimensions of fracture surfaces.

microstructural statistics, implies negligible probability of finding the dominant crack nucleus with further increase of the sample size. Consequently, the capability of the laboratory sample to capture the damage accumulation and failure of large engineering structures is directly related to the capability of controlling the inherent flaw structure of the brittle material on the spatial scale that dominates the dynamic response.

The simulation results indicate that the slope of power-law $\sigma_m \propto D^{-\varsigma}$, used typically to model the strength dependence of the sample size, is not significantly affected by strain rate in small-scale regime; an alternative approach is suggested to capture the clear strain-rate dependence. Simulation results also suggest that, as the sample size is reduced, the strain-rate effect is reduced as well, i.e., that the strain-rate governed increase of the tensile strength is less pronounced in the smaller brittle samples contrary to experimental observation in Cu nanopillars [22]. An empirical expression is proposed to model the sample size dependence upon the loading rate. The significant increase of strength data scatter with the sample-size reduction is clearly demonstrated, which is consistent with the brittle failures' inherent stochasticity and propensity for extreme value behavior. The results of the two-dimensional lattice simulations also indicate that the number of broken links corresponding to stress peak is described by a continuous spectrum of scaling exponents varying between 1 and 2 reflecting predominant damage distribution pattern.

Within the framework of this admittedly simple simulation model, the relations suggested are rather general, since no restrictions, with exception of the low fracture energy of micro-elements, are imposed on the properties of microstructure and microconstituents defining the model distributions. The discussed sample-size reduction is consistent with "the ordering effect of the kinetic energy" [10] reflected by transition from the random to deterministic dynamic response, attributed to the diminishing flaw sensitivity of the highly brittle materials with the loading rate increase.

ACKNOWLEDGMENT

Funding for this research was provided through the Serbian Ministry of Education and Science, under the grant OI 174010.

REFERENCES

[1] Bažant,Z.P. and Planas, J.: Fracture and Size Effect in Concrete and Other Quasibrittle Materials, CRC Press (1998)

[2] Breysse, D. and Renaudin, P.: On the influence of local disorder on size-effect, in: A. Carpinteri (Ed.), Size-Scale Effects in the Failure Mechanisms of Materials and Structures, E & FN Spon, London, (1996) pp. 187-199.

[3] Carpinteri, A., Chiaia, B. and Ferro, G.: Multifractal nature of material microstructure and size effects on nominal tensile strength, in: A. Baker, B.L. Karihaloo (Eds.), Fracture of Brittle Disordered Materials – Concrete, Rock and Ceramics, E & FN Spon, London, (1995) pp. 21-34.

[4] Curtin, W.A. and Scher, H.: Algebraic scaling of material strength. Phys. Rev. B, 45 (6), 2620-2627 (1992)

[5] Krajcinovic, D. and Rinaldi, A.: Thermodynamics and statistical physics of damage processes in quasi-ductile solids. Mech. Mater. 37, 299–315, (2005)

[6] Hansen, A, Roux, S. and Herrmann, H.J.: Rupture of central-force lattices. J. Phys. France 50, 733-744, (1989)

[7] Herrmann, H.J., Hansen, A. and Roux, S.: Fracture of disordered, elastic lattices in two dimensions. Phys. Rev. B 39 (1), 637-647, (1989)

[8] Krajcinovic, D.: Damage Mechanics, North-Holland, Amsterdam (1996)

[9] Monette, L. and Anderson, M.P.: Elastic and fracture properties of the two-dimensional triangular and square lattices. Modelling Simul. Mater. Sci. Eng., 2, 53-66 (1994)

[10] Mastilovic, S, Rinaldi, A. and Krajcinovic, D.: Ordering effect of kinetic energy on dynamic deformation of brittle solids. Mech. Mater, 40, 407-417 (2008)

[11] Mastilovic, S.: Some Observations Regarding Stochasticity of Dynamic Response of 2D Disordered Brittle Lattices. Int. J. Damage Mech., 20, 267-277 (2011)

[12] Rinaldi, A., Krajcnovic, D., and Mastilovic, S.: Statistical Damage Mechanics – Constitutive Relations. J. Theor. Appl. Mech., 44 (3), 585-602 (2006)

[13] Nemat-Nasser, S. And Hori, M.: Micromechanics: Overall Properties of Heterogeneous Materials. North-Holland, Amsterdam (1999)

[14] Qi, C., Wang, M., Qian, Q.: Strain rate effects on the strength and fragmentation size of rocks. Int. J. Impact Eng., 36, 1355-1364 (2009)

[15] Rinaldi, A. and Lai, Y.-C.: Statistical damage theory of 2D lattices: Energetics and physical foundations of damage parameter. Int. J. Plast., 23, 1796–1825 (2007)

[16] Rinaldi, A, Krajcinovic, D., Peralta, P, and Lai, Q.: Lattice models of polycrystalline microstructures: A quantitative approach. Mech. Mater, 40, 17-36 (2008)

[17] Del Piero, G. and Truskinovsky, L.: Macro- and micro-cracking in one-dimensional elasticity. Int. J. Solids Struct. 38, 1135-1148 (2001).

[18] Mastilovic, S.: A Note on Short-Time Response of Two-Dimensional Lattices During Dynamic Loading. Int. J. Damage Mech., 17, 357-361 (2008)

[19] Curtin, W.A. and Scher, H.: Brittle fracture in disordered materials: A spring network model. J. Mater. Res., 5 (3), 535-553 (1990)

[20] Mastilovic, S. and Krajcinovic, D.: Statistical Models of Brittle Deformation, Part Two: Computer Simulations. Int. J. Plast., 15, 427-456 (1999).

[21] Alibert, J.J., Seppecher, P., and Dell'Isola, F.: Truss Modular Beams with Deformation Energy depending on Higher Displacement Gradients. Math. Mech. Solids, 8: 51-73 (2003)

[22] Jennings, A.T., Li, J., and Greer, J.R.: Emergence of strain-rate sensitivity in Cu nanopillars: Transition from dislocation multiplication to dislocation nucleation. Acta Mater., 59, 5627–5637 (2011).

[23] Mastilovic, S.: Further Remarks on Stochastic Damage Evolution of Brittle Solids Under Dynamic Tensile Loading. Int. J. Damage Mech., 20, 900-921 (2011)

[24] Forest, S., Barbe, F., and Cailletaud, G.:. Cosserat modeling of size effects in the mechanical behavior of polycrystals and multi-phase materials. Int. J. Solids Struct., 37, 7105-7126 (2000).

[25] Delaplace, A., Pijaudier-Cabot, G, and Roux, S.:. Progressive damage in discrete models and consequences on continuum modeling. J. Mech. Phys. Solids, 44 (1), 99-136 (1996).

[26] Uchic, M.D., Dimiduk, D.M., Florando, J.N., and Nix. W.D.: Sample Dimensions Influence Strength and Crystal Plasticity. Science 305, 986-989 (2004).

[27] Greer, J.R., Oliver, W.C., Nix. W.D.: Size dependence of mechanical properties of gold at the micron scale in the absence of strain gradients. Acta Mater., 53, 1821-1830 (2005).

[28] Bei, H., Shim, S., Pharr, G.M., and George, E.P.: Effects of pre-strain on the compressive stress–strain response of Mo-alloy single-crystal micropillars. Acta Mater., 56, 4762–4770 (2008)

[29] Ng, K.S. and Ngan, A.H.W.: Stochastic nature of plasticity of aluminum micro-pillars. Acta Mater., 56, 1712–1720 (2008)

[30] Rinaldi, A., Peralta, P., Friesen, C., Nahar, D., Licoccia, S., Traversa, E. and Sieradzki, K.: Superhard Nanobuttons: Constraining Crystal Plasticity and Dealing with Extrinsic Effects at the Nanoscale. Small (2009)

[31] Kiener, D., Grosinger, W., Dehm, G., and Pippan, R.: A further step towards an understanding of size-dependent crystal plasticity: In situ tension experiments of miniaturized single-crystal copper samples. Acta Mater., 56, 580–592 (2008)

[32] Kim, J-Y., Jang, D. and Greer, J.R.: Tensile and compressive behavior of tungsten, molybdenum, tantalum and niobium at the nanoscale. Acta Mater., 58, 2355–2363 (2010)

[33] Dehm, G.: Miniaturized single-crystalline fcc metals deformed in tension: New insights in size-dependent plasticity. Progr. Mater. Sci., 54, 664–688 (2009)

[34] Uchic, M.D., Shade, P.A. and Dimiduk, D.M.: Plasticity of micrometer-scale single crystals in compression. Annu. Rev. Mater. Res., 39 (1), 361-386, (2009)

[35] Kraft, O., Gruber, P.A., Monig, R., and Weygand, D.: Plasticity in confined dimensions. Annu. Rev. Mater. Res., 40, 293-317 (2010)

[36] Greer, J.R. and De Hosson, J.Th.M.: Plasticity in small-sized metallic systems: Intrinsic versus extrinsic size effect. Progr. Mater. Sci., 56, 654–724 (2011)

[37] Tang, H., Schwarz, K.W. and Espinosa, H.D.: Dislocation escape-related size effects in single-crystal micropillars under uniaxial compression. Acta Mater. 55, 1607–1616 (2007)

[38] Rinaldi, A.: Effects of dislocation density and sample-size on plastic yielding at the nanoscale: a Weibull-like framework. Nanoscale, 3 (11), 4817-23, (2011)

[39] Rinaldi, A, Peralta, P., Sieradzki, K., Traversa, E., and Liccocio., S: Role of Dislocation Density on the Sample-Size Effect in Nanoscale Plastic Yielding. J. Nanomech. Micromech., doi:http://dx.doi.org/10.1061/(ASCE)NM.2153-5477.0000047

[40] Jagota, A., and Bennison, S.J.: Spring-Network and Finite Element Models for Elasticity and Fracture. Proceedings of a workshop on Breakdown and non-linearity in soft condensed matter. K.K. Bardhan, B.K. Chakrabarti, A. Hansen eds. Springer-Verlag Lecture Notes in Physics (Berlin, Heidelberg, New York) ISBN 3-540-58652-0. (1994)

[41] Van Vliet, M.R.A.: Size Effect in Tensile Fracture of Concrete and Rock. Delft University Press, Delft (2000)

[42] Mastilovic, S, Rinaldi, A. and Krajcinovic, D.: Ordering effect of kinetic energy on dynamic deformation of brittle solids. Mech. Mater, 40, 407-417 (2008)

[43] Morquio, A. and Riera, J.D.: Size and strain rate effects in steel structures. Engng. Struct., 26, 669-679, (2004)

[44] Hentz, S., Donz, F.V., and Daudeville, L.: Discrete element modelling of concrete submitted to dynamic loading at high strain rates, Comput. Struct., 82, 2509–2524, (2004)

[45] Cotsovos, D.M. and Pavlović, M.N.: Numerical investigation of concrete subjected to high rates of uniaxial tensile loading, Int. J. Impact Engng. 35, 319–335, (2008)

[46] Riera, J.D., Miguel, L.F.F. and Iturrioz, I: Strength of Brittle Materials under High Strain Rates in DEM Simulations, Comput. Model. Engng. Sci., 82 (2), 113-136, (2011)

[47] Ostoja-Starzewski, M.: Lattice models in micromechanics. Appl. Mech. Rev., 55 (1), 35-60, (2002)

[48] Castillo, E.: Extreme Value Theory in Engineering. Academic Press, Boston (1987)

[49] Mishnaevsky Jr., L.: Damage and Fracture in Heterogeneous Materials. *A.A.* Balkema, Rotterdam (1998)

[50] Hill, R.: Elastic properties of reinforced solids: Some theoretical principles. J. Mech. Phys. Solids 11, 357-372, (1963)

[51] Field, J.E., Walley, S.M., Proud, W.G., Goldrein, H.T. and Siviour, C.R.: Review of experimental techniques for high rate deformation and shock Studies. Int. J. Impact Eng. 30 (2000)

[52] Bourne, N.K.: Materials' Physics in Extremes: Akrology. Metallurgical and materials Transactions A, 42, 2975-2984 (2011)

[53] Lawn, B.: Fracture of Brittle Solids, second ed.. Cambridge University Press, Cambridge, (1993)

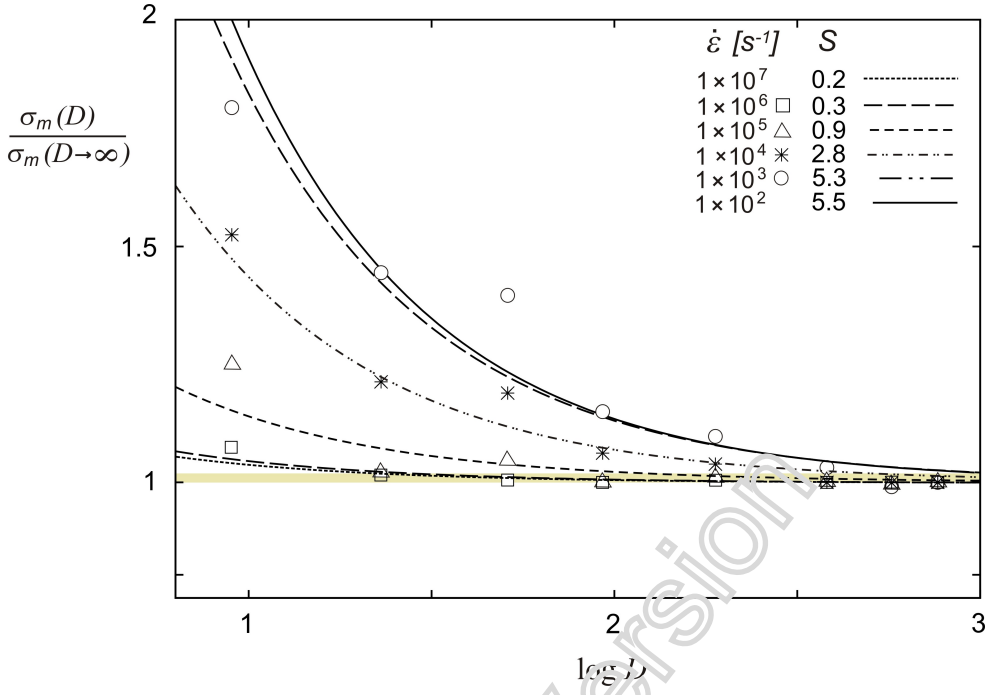

Figure 1. Examples of the rate-dependent tensile strength size effect; one $(\dot{\varepsilon}, D)$ realization. The sample size D is, hereinafter, normalized by the resolution length, l_c, for brevity. (The curves represent the least-squares data fit. S parameter is defined in relation with Eq. (4b) with scaling exponent n=0.8).

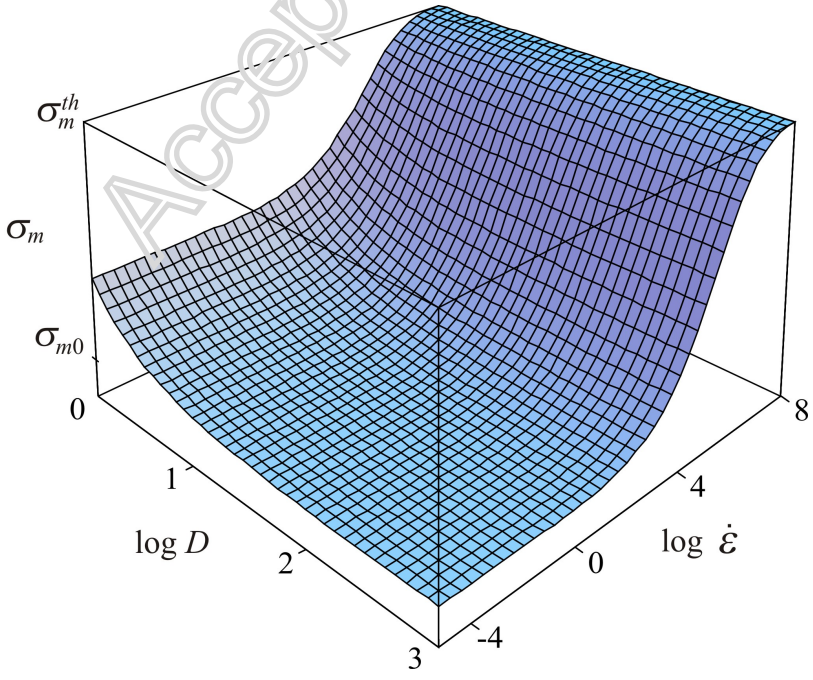

Figure. 2 Schematic representation of the tensile strength dependence on the strain rate and the sample size.

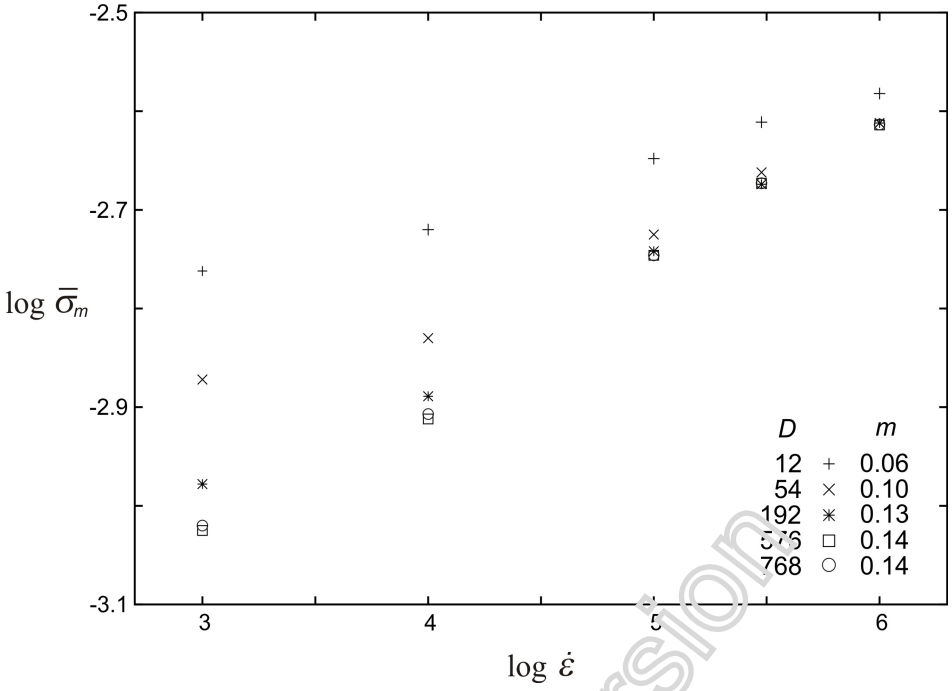

Figure. 3 Sample-size dependence of the strain-rate driven tensile strength increase. The strength is normalized by the modulus of elasticity of pristine material, $\bar{\sigma}_m = \sigma_m / E_0$. The strain-rate sensitivity parameter m refers to the commonly used empirical equation $\sigma_m = \sigma_0 \dot{\varepsilon}^m$.

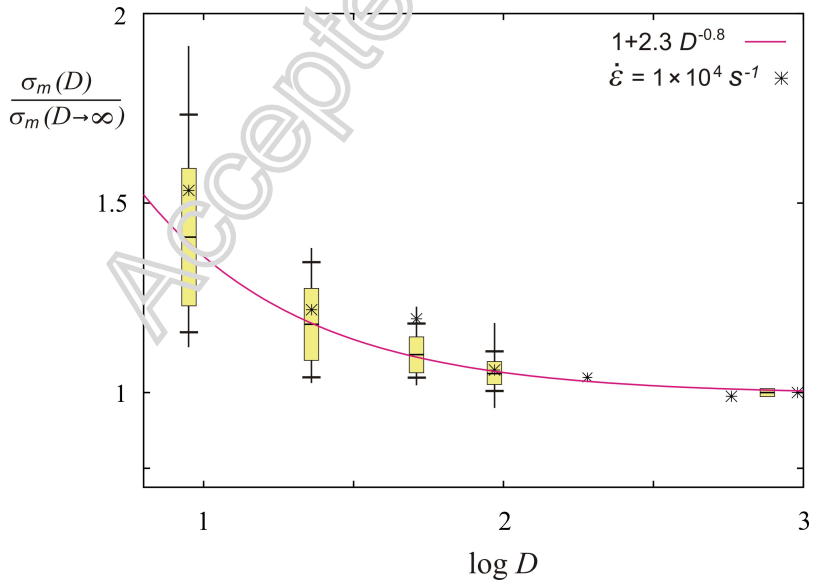

Figure. 4 The basic statistics of size-dependent tensile strength increase for $\dot{\varepsilon} = 1\times10^4\ s^{-1}$. The rectangles outline the mean value +/- the standard deviation. The horizontal lines depict the non-outlier maximum and minimum values while the vertical line extends to the minimum and maximum of the complete data set. The asterisk denotes the corresponding values for a single realization presented in Fig. 1. The curves represent the least-squares data fit (S=2.3 and ζ=0.8).

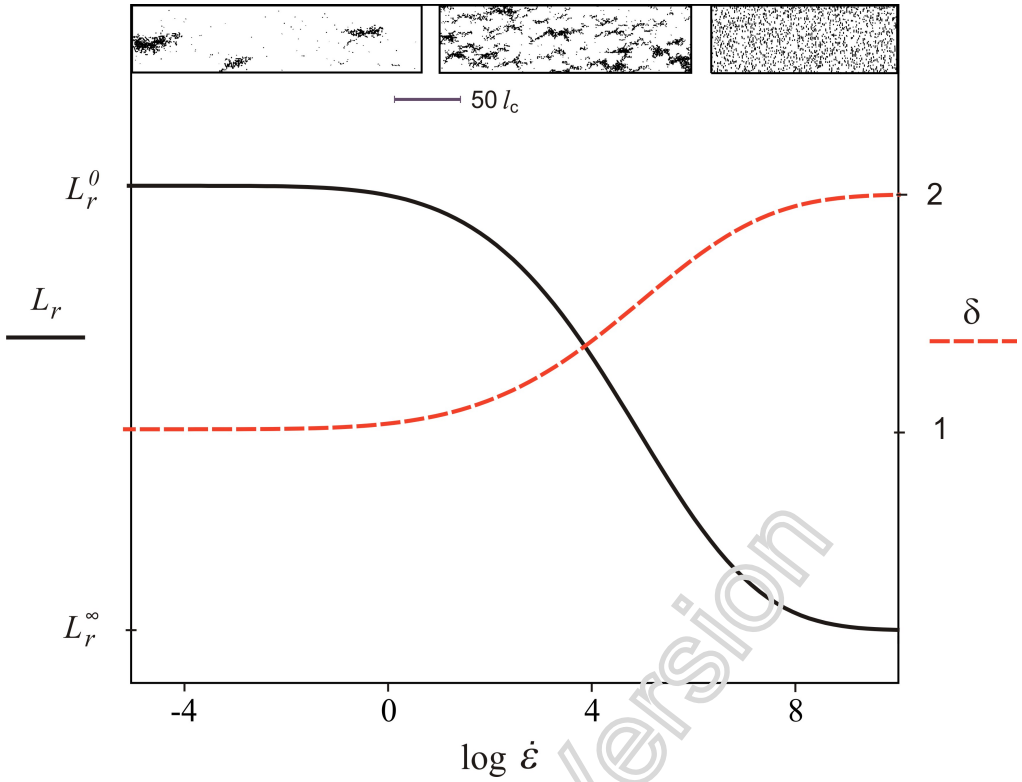

Figure. 5: Schematic representation of the strain rate effect on the representative sample size (L_r) and the stress-peak broken bonds scaling exponent (δ), and corresponding typical damage pattern types. (The damage patterns, added to facilitate the discussion, are sample details typical of the softening phase in the low-medium, transitional (high), and extremely high strain-rate regions (for more detail see [10, 23]).)

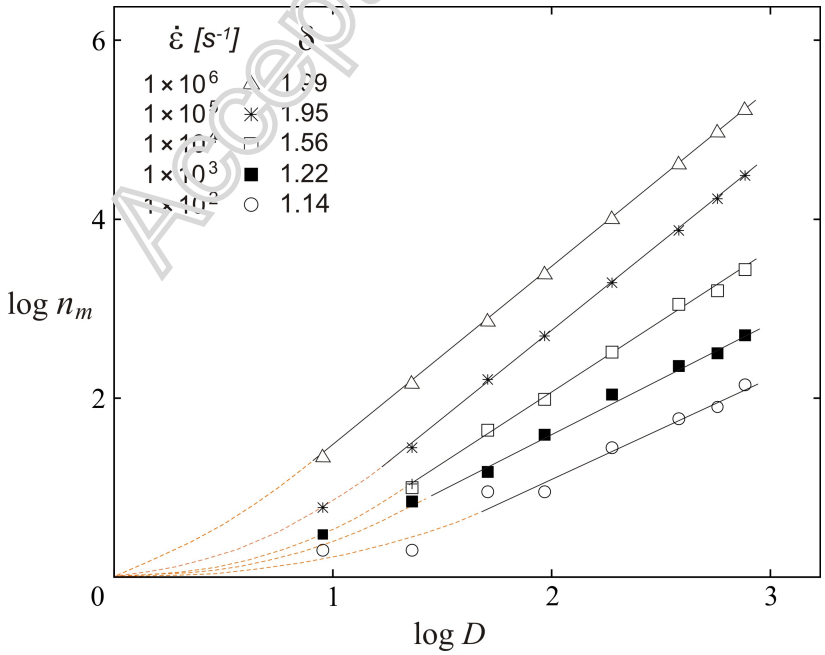

Figure.6: Variation of the stress-peak number of broken links with the lattice size for different strain rates of the transitory region. (The straight lines represent the least-squares data fit).